LETTER

doi:10.1038/nature11674

COUP-TFII inhibits TGF-β-induced growth barrier to promote prostate tumorigenesis

Jun Qin[1], San-Pin Wu[1], Chad J. Creighton[2], Fangyan Dai[1,3], Xin Xie[1], Chiang-Min Cheng[1], Anna Frolov[4], Gustavo Ayala[4]†, Xia Lin[3], Xin-Hua Feng[1,3], Michael M. Ittmann[4], Shaw-Jenq Tsai[1,5], Ming-Jer Tsai[1,6] & Sophia Y. Tsai[1,6]

Mutations in phosphatase and tensin homologue (PTEN) or genomic alterations in the phosphatidylinositol-3-OH kinase-signalling pathway are the most common genetic alterations reported in human prostate cancer[1–4]. However, the precise mechanism underlying how indolent tumours with PTEN alterations acquire metastatic potential remains poorly understood. Recent studies suggest that upregulation of transforming growth factor (TGF)-β signalling triggered by PTEN loss will form a growth barrier as a defence mechanism to constrain prostate cancer progression[5], underscoring that TGF-β signalling might represent a pre-invasive checkpoint to prevent PTEN-mediated prostate tumorigenesis. Here we show that COUP transcription factor II (COUP-TFII, also known as NR2F2)[6–9], a member of the nuclear receptor superfamily, serves as a key regulator to inhibit SMAD4-dependent transcription, and consequently overrides the TGF-β-dependent checkpoint for PTEN-null indolent tumours. Overexpression of COUP-TFII in the mouse prostate epithelium cooperates with PTEN deletion to augment malignant progression and produce an aggressive metastasis-prone tumour. The functional counteraction between COUP-TFII and SMAD4 is reinforced by genetically engineered mouse models in which conditional loss of SMAD4 diminishes the inhibitory effects elicited by COUP-TFII ablation. The biological significance of COUP-TFII in prostate carcinogenesis is substantiated by patient sample analysis, in which COUP-TFII expression or activity is tightly correlated with tumour recurrence and disease progression, whereas it is inversely associated with TGF-β signalling. These findings reveal that the destruction of the TGF-β-dependent barrier by COUP-TFII is crucial for the progression of PTEN-mutant prostate cancer into a life-threatening disease, and supports COUP-TFII as a potential drug target for the intervention of metastatic human prostate cancer.

COUP-TFII is known to promote tumour angiogenesis through its function in the tumour microenvironment[10,11], but its role in tumour cells remains undefined. Consistent with aberrant expression of COUP-TFII reported in various tumours[12–17], Oncomine expression analysis revealed higher COUP-TFII expression in prostate tumour cells and in metastatic prostate cancer than in primary prostate cancer[12,13] (Supplementary Fig. 1a). To assess the clinical relevance of COUP-TFII in human prostate cancer, we stained for COUP-TFII in a tumour tissue microarray (TMA) consisting of 407 patient specimens. Examination of clinical prostate specimens showed higher levels of COUP-TFII expression in prostate tumour cells in comparison to the adjacent normal prostate epithelium (Supplementary Fig. 1b). As summarized in Fig. 1a, approximately 60% of human prostate cancer specimens exhibited intermediate to intense nuclear COUP-TFII staining, whereas only 5% of normal prostate epithelial cells stained positive for COUP-TFII. Further correlation studies indicated that COUP-TFII expression in tumour cells significantly associated with pathological predictors of human prostate cancer aggressiveness (Supplementary Table 1). Most importantly, univariate analysis indicated that COUP-TFII expression levels in prostate tumour cells could serve as a predictor to stratify risk of recurrence in patients; patients bearing higher levels of COUP-TFII expression showed earlier recurrence after radical prostatectomy (Fig. 1b). Cox proportional hazards regression analyses showed that tumour recurrence was sensitive to gradual increases of COUP-TFII expression levels, as reflected by the increasing hazard ratios, from 1.5 to 1.8 and 2.5.

These results prompted us to use genetically engineered mouse models to determine the causal role of COUP-TFII in prostate tumorigenesis. As such, we engineered mice containing PB-Cre (the *Cre* gene under control of the prostate-specific probasin promoter)[18] and conditional knockout alleles of *Pten*[3] and/or *COUP-TFII* (also known as *Nr2f2*)[7], hereafter referred to as $Pten^{PC-/-}$ and $Pten^{PC-/-}$; $COUP\text{-}TFII^{PC-/-}$ mice, respectively (Supplementary Fig. 2a, b). PTEN-null mice lacking COUP-TFII exhibited a significant reduction in prostate weight (Supplementary Fig. 2c), suggesting a positive role for COUP-TFII in driving prostate tumorigenesis. Histopathological analysis of

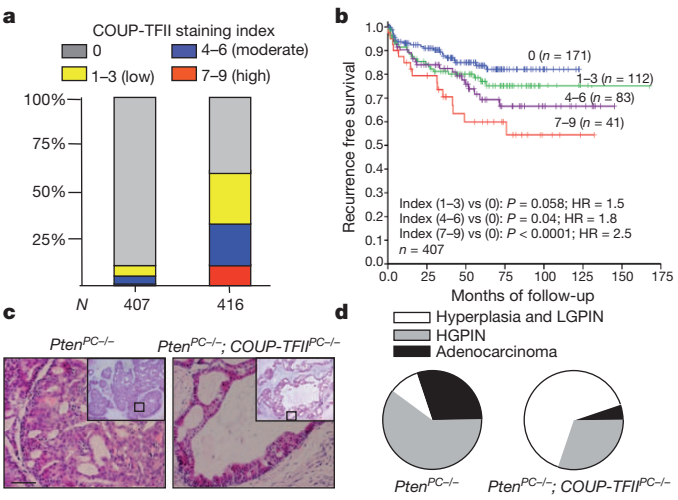

Figure 1 | COUP-TFII is crucial for prostate cancer progression in human and mice. a, Expression and clinical relevance of COUP-TFII are assessed in a human prostate cancer TMA. COUP-TFII staining indexes in cohorts of normal prostate epithelial cells ($n = 407$) and prostate tumours ($n = 416$) are shown as stacked columns. **b**, Kaplan–Meier plot of the recurrence after radical prostatectomy based on the COUP-TFII expression index in patients. HR, hazard ratio. **c**, Haematoxylin and eosin (H&E) staining of the anterior prostate from $Pten^{PC-/-}$ and $Pten^{PC-/-}$; $COUP\text{-}TFII^{PC-/-}$ mice at 5 months of age. Scale bar, 50 μm. **d**, Pie graphs show prostate tumour progressions in $Pten^{PC-/-}$ and $Pten^{PC-/-}$; $COUP\text{-}TFII^{PC-/-}$ mice (5 months old; $n = 10$). HGPIN, high-grade PIN; LGPIN, low-grade PIN.

[1]Department of Molecular and Cellular Biology, Baylor College of Medicine, Houston, Texas 77030, USA. [2]Dan L. Duncan Cancer Center, Baylor College of Medicine, Houston, Texas 77030, USA. [3]Michael E. DeBakey Department of Surgery, Baylor College of Medicine, Houston, Texas 77030, USA. [4]Department of Pathology and Immunology, Baylor College of Medicine, Houston, Texas 77030, USA. [5]Department of Physiology, College of Medicine, National Cheng Kung University, Tainan 701, Taiwan. [6]Program in Developmental Biology, Baylor College of Medicine, Houston, Texas 77030, USA. †Present address: Department of Pathology and Laboratory Medicine, University of Texas Health Science Center Medical School, Houston, Texas 77030, USA.

the entire animal cohort showed that loss of COUP-TFII compromised prostate tumour progression, as reflected by the arrest of tumours at the hyperplastic or low-grade prostatic intraepithelial neoplasia (PIN) stage at 5 months of age, whereas tumours from *Pten*$^{PC-/-}$ mice already advanced to high-grade PIN or adenocarcinoma (Fig. 1c, d and Supplementary Fig. 2d). The normal prostatic histology in *COUP-TFII*$^{PC-/-}$ mice (Supplementary Fig. 2e) argued against a possibility that it was due to a developmental defect. Moreover, loss of COUP-TFII attenuated the proliferation advantage elicited by PTEN loss, whereas the levels of angiogenesis remained similar and thus is unlikely to have contributed to the restriction of prostate tumorigenesis (Supplementary Fig. 2f, g).

Given that COUP-TFII was further upregulated in metastatic prostate cancer, and its higher expression correlated with a worse clinical outcome, we sought to determine whether overexpression of COUP-TFII in PTEN-null tumours would exacerbate prostate tumorigenesis. As such, we generated an inducible COUP-TFII overexpression mouse, *COUP-TFII*$^{OE/+}$ (Fig. 2a), that allows constitutive COUP-TFII expression in the prostate epithelium. During 12 months of follow-up, *COUP-TFII*$^{OE/+}$ mice exhibited normal prostatic histology (Supplementary Fig. 3a), indicating that COUP-TFII by itself is not sufficient to initiate prostate neoplasia, and that cooperating oncogenic lesions are required. Indeed, overexpression of COUP-TFII in a PTEN-heterozygous background resulted in a rapid acceleration of tumour progression, with overt and high penetrance PIN starting at 4 months of age and progressing to high-grade PIN or adenocarcinoma by 12 months (Fig. 2b). These data demonstrate that COUP-TFII enables rapid disease progression from preneoplastic prostatic epithelium.

Next, we determined whether prostate-specific overexpression of COUP-TFII in a PTEN-null background would produce a metastasis-prone cancer. By 24 weeks of age, *Pten*$^{PC-/-}$; *COUP-TFII*$^{OE/+}$ mice developed highly aggressive carcinoma with an altered stroma, as evidenced by the attenuation or loss of the periglandular smooth muscle layer and androgen receptor (AR)-positive tumour cells invading into the stroma (Fig. 2c), in which subsets of invasive tumour cells exhibited epithelial–mesenchymal transition (Supplementary Fig. 3c). Molecular pathological analysis of prostate-cancer-bearing *Pten*$^{PC-/-}$; *COUP-TFII*$^{OE/+}$ mice also showed a metastatic spread of AR-positive tumour nodules to lumbar lymph nodes in 13 out of 16 cases, and lung metastasis in 4 out of 16 cases (Fig. 2d). By contrast, *Pten*$^{PC-/-}$ mice only showed a modest metastatic phenotype[2–4]. Even with more aggressive tumour phenotypes, angiogenesis was not altered whereas proliferation was enhanced after COUP-TFII overexpression (Fig. 2e and Supplementary Figs 3d, e and 4). Collectively, COUP-TFII overexpression enhances the full spectrum of prostate cancer development, leading to aggressive metastasis in PTEN-null tumours.

To determine how COUP-TFII affects tumorigenesis, we conducted a transcriptome comparison using COUP-TFII-depleted PC3 cells. Unbiased ingenuity pathway analysis indicated that COUP-TFII was crucial for the growth of human prostate cancer cells, an observation reinforced by anchorage-independent growth assays and cell proliferation/viability tests (MTT assay) (Supplementary Fig. 5). Further gene-set enrichment analysis and comparison with our gene expression profile to a defined TGF-β response signature[19] indicated a global enrichment of TGF-β-induced genes in the absence of COUP-TFII (Fig. 3a and Supplementary Fig. 6a). Given that TGF-β signalling is crucial for prostate cancer progression[5,20], we examined whether COUP-TFII potentiated prostate tumorigenesis through TGF-β signalling. In human prostate cancer cells, COUP-TFII served as a transcriptional inhibitor of TGF-β signalling (Supplementary Fig. 6b–d). Knockdown of COUP-TFII in PC3 cells substantially altered p21, p15 and cyclin D1 expression in response to TGF-β stimulation (Supplementary Fig. 6e). Protein levels of p21 were also increased without TGF-β stimulation, presumably owing to autocrine TGF-β signalling in PC3 cells (Supplementary Fig. 6f).

We postulated that overexpression of COUP-TFII enabled the indolent PTEN-null tumours to acquire metastatic potential through the destruction of a TGF-β-induced growth barrier. Indeed, in

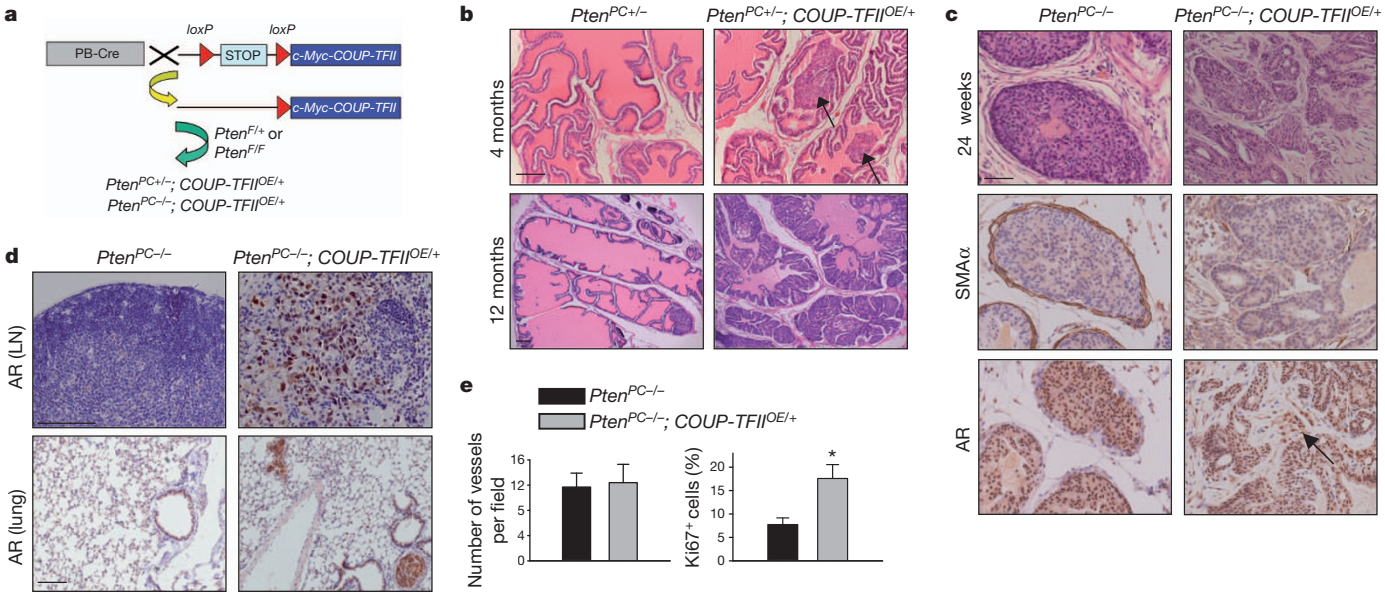

Figure 2 | Prostate-specific overexpression of COUP-TFII promotes tumorigenesis in PTEN mutated mice. **a**, Scheme of conditional overexpression of COUP-TFII (*Rosa26-lox-STOP-lox-COUP-TFII; COUP-TFII*$^{OE/+}$) in a PTEN spontaneous tumour model. *COUP-TFII*$^{OE/+}$ mice contain a single copy of a mini gene, consisting of a CAGGS promoter, a *loxP*-STOP-*loxP* (LSL) cassette and Myc-tagged *COUP-TFII* complementary DNA, knocked into the ROSA locus. In the presence of PB-Cre recombinase, the LSL cassette is excised, allowing COUP-TFII expression in the prostate epithelium. **b**, H&E-stained sections of representative anterior prostate at 4 and 12 months of age in *Pten*$^{PC+/-}$ and *Pten*$^{PC+/-}$; *COUP-TFII*$^{OE/+}$ mice. Arrows indicate PIN. **c**, H&E-stained sections of anterior prostate at 24 weeks of age in *Pten*$^{PC-/-}$ and *Pten*$^{PC-/-}$; *COUP-TFII*$^{OE/+}$ mice (top). Immunohistochemistry of α-smooth muscle actin (SMAα) (middle) and AR (bottom) expression. **d**, Immunohistochemical staining of AR expression in lumbar lymph nodes (LN) and lung from 6-month-old *Pten*$^{PC-/-}$ and *Pten*$^{PC-/-}$; *COUP-TFII*$^{OE/+}$ mice. **e**, Semi-quantitative results of Ki67 and CD31 staining of prostate tumours from 6-month-old *Pten*$^{PC-/-}$ and *Pten*$^{PC-/-}$; *COUP-TFII*$^{OE/+}$ mice $n = 6$ (**b**–**e**); $^*P < 0.05$. Data are mean and s.e.m. Scale bars, 100 μm (**b**, **d**) and 50 μm (**c**).

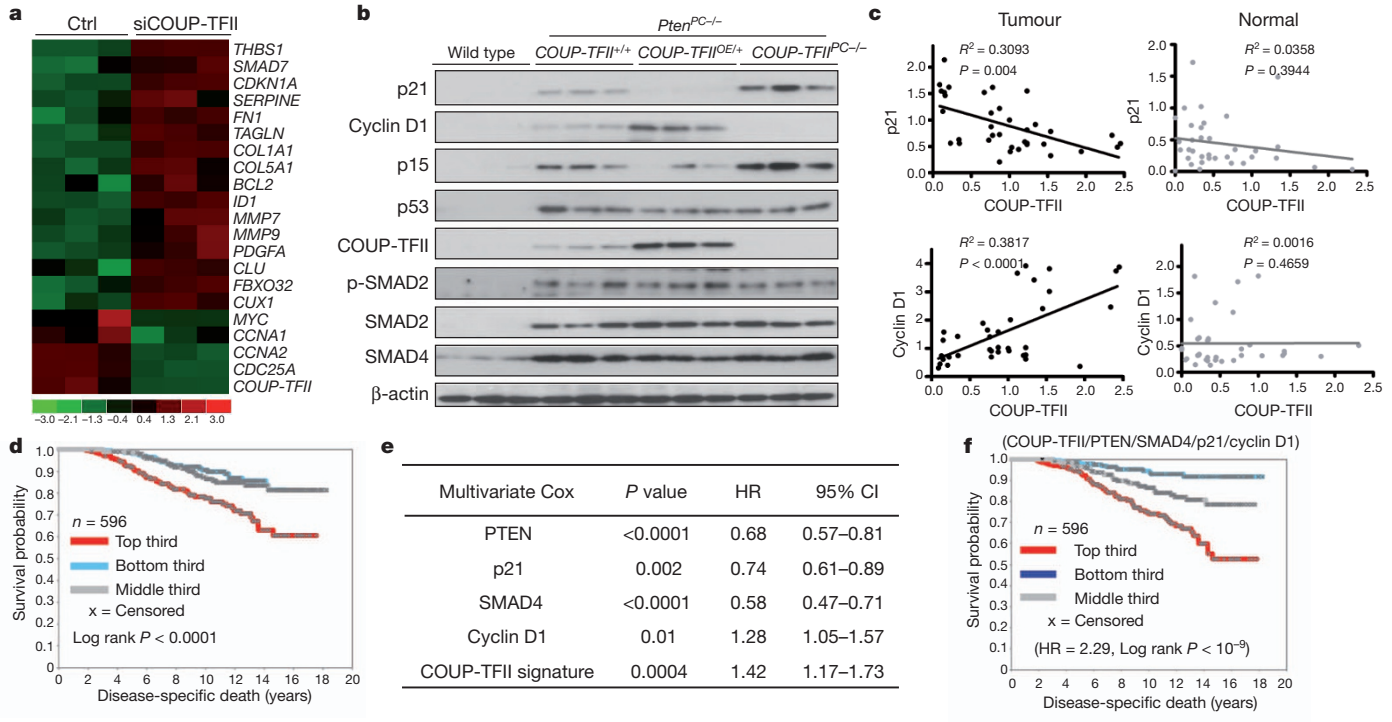

Multivariate Cox	*P* value	HR	95% CI
PTEN	<0.0001	0.68	0.57–0.81
p21	0.002	0.74	0.61–0.89
SMAD4	<0.0001	0.58	0.47–0.71
Cyclin D1	0.01	1.28	1.05–1.57
COUP-TFII signature	0.0004	1.42	1.17–1.73

Figure 3 | COUP-TFII inhibits TGF-β signalling in prostate cancer cells. **a**, Heat map of microarray results shows the enrichment of TGF-β downstream target genes in COUP-TFII-depleted PC3 cells. siCOUP-TFII denotes COUP-TFII short interfering RNA (siRNA); ctrl denotes control. **b**, Western blot analysis of core regulators and downstream targets of TGF-β signalling, as well as p53, in anterior prostates from 24-week-old mice as indicated. **c**, The correlation between COUP-TFII and TGF-β signalling targets (p21 and cyclin D1) in patient prostate tumours and normal prostate counterparts are shown in regression plots ($n = 36$). **d**–**f**, Association of COUP-TFII gene signature with disease-specific death in patients with prostate cancer using data set GSE10645. **d**, Kaplan–Meier plot, with top third, middle third and bottom third of patients representing COUP-TFII activities from high to low (*P* value by log-rank test). **e**, Multivariate Cox regression analysis of COUP-TFII signature and the transcription levels of PTEN, SMAD4, p21 and cyclin D1. **f**, Kaplan–Meier plot of patients grouped using the combination of COUP-TFII and PTEN/SMAD4/cyclin D1/p21 gene sets.

$Pten^{PC-/-}$; $COUP\text{-}TFII^{OE/+}$ mice, the TGF-β-induced growth barrier was significantly attenuated after increased COUP-TFII expression (Fig. 3b). Overexpression of COUP-TFII profoundly neutralized oncogene-induced senescence, as judged by the reduction of senescence-associated β-galactosidase staining (Supplementary Fig. 6g), whereas ablation of COUP-TFII in PTEN-null mice enhanced the acquisition of hyperactivity of TGF-β signalling and a marked induction in cellular senescence. Furthermore, the clinical relevance between COUP-TFII levels and TGF-β signalling activities was established by a significant correlation between COUP-TFII and p21/cyclin D1 expression in prostate tumours, but not in normal prostate epithelium counterparts, in a cohort of 36 patients with highly aggressive prostate cancer (Fig. 3c).

Next, we extended our findings by querying the gene expression profiling data set GSE10645 (ref. 21) that contains 596 primary human tumours with prostate cancer-specific death information, to complement our TMA results. Using gene expression profiles obtained in PC3 cells, we found a total of 80 COUP-TFII-regulated genes represented in GSE10645 (Methods, Supplementary Fig. 7 and Supplementary Table 2); the genes were used to score each of the human tumours for COUP-TFII activity. We observed distinct differences in the time to prostate-cancer-specific death, although no differences in the time to prostate-specific antigen (PSA) recurrence, among the patients with higher versus lower COUP-TFII activity (Fig. 3d and Supplementary Table 3–5). Multivariate Cox model analysis indicated that the PTEN, SMAD4, p21, cyclin D1 and COUP-TFII signature (Methods) all independently provided predictive power to stratify patients into high- and low-risk groups (Fig. 3e). Plotting the combined transcript levels of PTEN, SMAD4, p21 and cyclin D1 together with the higher COUP-TFII signature in prostatectomies increased the predictive power from that of either gene set alone (Fig. 3f), illustrating a significant genetic cooperation between COUP-TFII and TGF-β signalling in PTEN-null human prostate cancer tumours.

Because depletion of COUP-TFII failed to affect the levels of SMAD2/3/4, the receptors or the activated form of phosphorylated-SMAD2/3 (Supplementary Fig. 8), we investigated whether COUP-TFII could interact directly with any of these SMAD proteins. Indeed, COUP-TFII strongly associated with SMAD4 in cells (Supplementary Fig. 9a–c) and in patient tumour specimens (Fig. 4a). Overexpression of mutant COUP-TFII-M2, which was unable to associate with SMAD4, failed to inhibit TGF-β signalling, indicating that the COUP-TFII–SMAD4 interaction was essential for the COUP-TFII effects on TGF-β signalling (Supplementary Fig. 9d–f). Mechanistically, our data indicated that COUP-TFII sequestered SMAD4 from binding to TGF-β-target gene promoters in cells (Supplementary Fig. 10) and in tumours containing higher levels of COUP-TFII (Fig. 4b).

As supporting evidence for the counteraction between COUP-TFII and SMAD4, knockdown of SMAD4 in PC3 cells alleviated the proliferative defects exerted by COUP-TFII depletion (Supplementary Fig. 11). Furthermore, we used a SMAD4 conditional knockout mouse[22] to examine the tumour spectrum in $Pten^{PC-/-}$; $COUP\text{-}TFII^{PC-/-}$ and $Pten^{PC-/-}$; $COUP\text{-}TFII^{OE/+}$ mice. Compared with hyperplasia or low-grade PIN lesions observed in 5-month-old $Pten^{PC-/-}$; $COUP\text{-}TFII^{PC-/-}$ mice, ablation of SMAD4 in COUP-TFII-null mice restored the full spectrum of tumour development as evidenced by the abundance of Ki67-labelled nuclei, the appearance of microinvasive tumours and the similar incidences of lymph node metastasis between $Pten^{PC-/-}$; $Smad4^{PC-/-}$ and $Pten^{PC-/-}$; $COUP\text{-}TFII^{PC-/-}$; $Smad4^{PC-/-}$ mice (Fig. 4c, d and Supplementary Figs 12–14). Moreover, overexpression of COUP-TFII in $Pten^{PC-/-}$; $Smad4^{PC-/-}$ mice did not further aggravate the invasive phenotypes displayed by the $Pten^{PC-/-}$; $Smad4^{PC-/-}$ mice (Fig. 4c, d and Supplementary Figs 12–14).

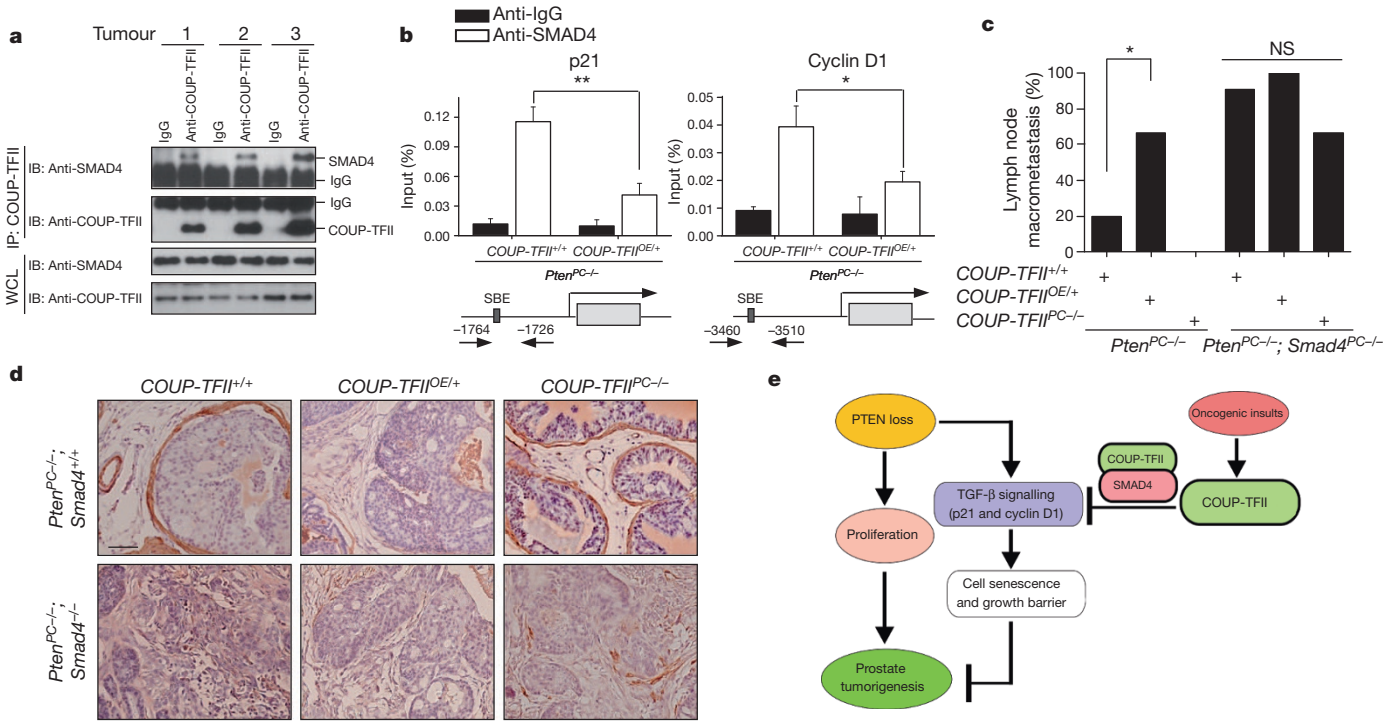

Figure 4 | COUP-TFII interacts with SMAD4 to modulate TGF-β signalling. **a**, Co-immunoprecipitation (IP) analysis of COUP-TFII and SMAD4 association in human prostate tumour specimens. IB, immunoblot. **b**, Cell lysates were prepared from prostate tumours in $Pten^{PC-/-}$ and $Pten^{PC-/-}$; $COUP\text{-}TFII^{OE/+}$ mice (6 months of age, $n = 3$), and subjected to chromatin immunoprecipitation analysis of SMAD4 binding at the p21 or cyclin D1 promoter. **c**, **d**, Analyses of the lymph node metastasis (**c**) and SMAα expression (**d**) in prostate tumours from $Pten^{PC-/-}$, $Pten^{PC-/-}$; $COUP\text{-}TFII^{OE/+}$, $Pten^{PC-/-}$; $COUP\text{-}TFII^{PC-/-}$ mice with or without SMAD4 deletion (5 months of age). **e**, Model of COUP-TFII in prostate tumorigenesis. PTEN inactivation drives prostate tumour initiation and progression. However, it also elicits the activation of TGF-β signalling that induces cellular senescence to constrain the indolent tumour from becoming aggressive. To develop metastasis-prone tumours, alternative oncogenic signals stimulate COUP-TFII expression, which counteracts the TGF-β-dependent checkpoint through direct association with SMAD4. Thus, COUP-TFII serves as a crucial regulator that counteracts the TGF-β-dependent growth barrier to enable indolent prostate cancer tumours to acquire metastatic potential. $*P < 0.05$; $**P < 0.01$. Data in **b** and **c** are mean and s.e.m.

In summary, our findings highlight a crucial role for COUP-TFII in driving full malignant progression of PTEN-null prostate tumorigenesis by counteracting TGF-β negative feedback signalling (Fig. 4e). As COUP-TFII is a member of the nuclear receptor family, the activity of which can be regulated by small molecules[23], our studies provide a potential new drug target for the intervention of metastatic human prostate cancer.

METHODS SUMMARY

Tissue microarrays used in this study were described previously[24,25]. All animal experiments were approved by the Animal Center for Comparative Medicine at Baylor College of Medicine. Detailed materials, methods and statistical analysis are provided in the Methods.

Full Methods and any associated references are available in the online version of the paper.

Received 5 December 2011; accepted 10 October 2012.
Published online 28 November 2012.

1. Taylor, B. S. *et al.* Integrative genomic profiling of human prostate cancer. *Cancer Cell* **18,** 11–22 (2010).
2. Trotman, L. C. *et al.* Pten dose dictates cancer progression in the prostate. *PLoS Biol.* **1,** E59 (2003).
3. Wang, S. *et al.* Prostate-specific deletion of the murine Pten tumor suppressor gene leads to metastatic prostate cancer. *Cancer Cell* **4,** 209–221 (2003).
4. Chen, Z. *et al.* Crucial role of p53-dependent cellular senescence in suppression of Pten-deficient tumorigenesis. *Nature* **436,** 725–730 (2005).
5. Ding, Z. *et al.* SMAD4-dependent barrier constrains prostate cancer growth and metastatic progression. *Nature* **470,** 269–273 (2011).
6. Pereira, F. A., Qiu, Y., Zhou, G., Tsai, M. J. & Tsai, S. Y. The orphan nuclear receptor COUP-TFII is required for angiogenesis and heart development. *Genes Dev.* **13,** 1037–1049 (1999).
7. Takamoto, N. *et al.* COUP-TFII is essential for radial and anteroposterior patterning of the stomach. *Development* **132,** 2179–2189 (2005).
8. You, L. R. *et al.* Suppression of Notch signalling by the COUP-TFII transcription factor regulates vein identity. *Nature* **435,** 98–104 (2005).
9. Lin, F. J., Qin, J., Tang, K., Tsai, S. Y. & Tsai, M. J. Coup d'Etat: an orphan takes control. *Endocr. Rev.* **32,** 404–421 (2011).
10. Qin, J., Chen, X., Yu-Lee, L. Y., Tsai, M. J. & Tsai, S. Y. Nuclear receptor COUP-TFII controls pancreatic islet tumor angiogenesis by regulating vascular endothelial growth factor/vascular endothelial growth factor receptor-2 signaling. *Cancer Res.* **70,** 8812–8821 (2010).
11. Qin, J., Chen, X., Xie, X., Tsai, M. J. & Tsai, S. Y. COUP-TFII regulates tumor growth and metastasis by modulating tumor angiogenesis. *Proc. Natl Acad. Sci. USA* **107,** 3687–3692 (2010).
12. Dhanasekaran, S. M. *et al.* Delineation of prognostic biomarkers in prostate cancer. *Nature* **412,** 822–826 (2001).
13. Tomlins, S. A. *et al.* Integrative molecular concept modeling of prostate cancer progression. *Nature Genet.* **39,** 41–51 (2007).
14. Nagasaki, S. *et al.* Chicken ovalbumin upstream promoter transcription factor II in human breast carcinoma: possible regulator of lymphangiogenesis via vascular endothelial growth factor-C expression. *Cancer Sci.* **100,** 639–645 (2009).
15. Shin, S. W. *et al.* Clinical significance of chicken ovalbumin upstream promoter-transcription factor II expression in human colorectal cancer. *Oncol. Rep.* **21,** 101–106 (2009).
16. Dyrskjøt, L. *et al.* Gene expression in the urinary bladder: a common carcinoma in situ gene expression signature exists disregarding histopathological classification. *Cancer Res.* **64,** 4040–4048 (2004).
17. Yeh, H. Y. *et al.* Identifying significant genetic regulatory networks in the prostate cancer from microarray data based on transcription factor analysis and conditional independency. *BMC Med. Genomics* **2,** 70 (2009).
18. Jin, C., McKeehan, K. & Wang, F. Transgenic mouse with high Cre recombinase activity in all prostate lobes, seminal vesicle, and ductus deferens. *Prostate* **57,** 160–164 (2003).
19. Padua, D. *et al.* TGFβ primes breast tumors for lung metastasis seeding through angiopoietin-like 4. *Cell* **133,** 66–77 (2008).
20. Chen, M. *et al.* Identification of PHLPP1 as a tumor suppressor reveals the role of feedback activation in PTEN-mutant prostate cancer progression. *Cancer Cell* **20,** 173–186 (2011).

21. Nakagawa, T. *et al.* A tissue biomarker panel predicting systemic progression after PSA recurrence post-definitive prostate cancer therapy. *PLoS ONE* **3,** e2318 (2008).
22. Chu, G. C., Dunn, N. R., Anderson, D. C., Oxburgh, L. & Robertson, E. J. Differential requirements for Smad4 in TGFβ-dependent patterning of the early mouse embryo. *Development* **131,** 3501–3512 (2004).
23. Kruse, S. W. *et al.* Identification of COUP-TFII orphan nuclear receptor as a retinoic acid-activated receptor. *PLoS Biol.* **6,** e227 (2008).
24. Ayala, G. *et al.* High levels of phosphorylated form of Akt-1 in prostate cancer and non-neoplastic prostate tissues are strong predictors of biochemical recurrence. *Clin. Cancer Res.* **10,** 6572–6578 (2004).
25. Hodgson, M. C. *et al.* Decreased expression and androgen regulation of the tumor suppressor gene INPP4B in prostate cancer. *Cancer Res.* **71,** 572–582 (2011).

Supplementary Information is available in the online version of the paper.

Acknowledgements We thank H. Wu for the *Pten*$^{flox/flox}$ mice, F. Wang for *ARR2PB-Cre* (PB-Cre) transgenic mice and E. J. Robertson for the *Smad4*$^{flox/flox}$ mice. We thank H. K. Graves and L.-Y. Yu-Lee for editorial assistance and S. Elledge for comments. We also thank the Baylor Microarray Core supported by the DERC Center (P30 DK079638) for the microarray analysis. This work was supported by grants from the National Institutes of Health DK62434, DK59820 (S.Y.T. and M.-J.T.), DK45641 (M.-J.T.) and HL76448 (S.Y.T.), and the Dan L. Duncan Cancer Center.

Author Contributions J.Q., M.-J.T. and S.Y.T. conceived and designed the experimental approach, performed experiments and prepared the manuscript as senior authors. C.J.C. contributed to computational analysis for gene signature analysis and statistical analysis. A.F., G.A. and M.M.I. performed TMA and pathology analyses. S.-P.W. generated *COUP-TFII*$^{OE/+}$ mice. F.D., X.X. and C.-M.C. performed and X.-H.F., X.L. and S.-J.T. supervised a specific subset of experimental design and analysis.

Author Information The microarray data have been deposited in the Gene Expression Omnibus (GEO) database under accession number GSE33182. Reprints and permissions information is available at www.nature.com/reprints. The authors declare no competing financial interests. Readers are welcome to comment on the online version of the paper. Correspondence and requests for materials should be addressed to M.J.T. (mtsai@bcm.edu) or S.Y.T. (stsai@bcm.edu).

METHODS

Immunohistochemistry and quantitative reverse transcriptase PCR analysis. Tissue microarrays used in this study were described previously[24,25]. Samples were procured from radical prostatectomies of 416 patients, who received no adjuvant therapy such as radiation or hormonal therapy. Other patient characteristics were as described previously[24–26]. Immunohistochemical analyses were done as described[24–26] using a specific anti-COUP-TFII antibody (Perseus Proteomics). Samples were scanned using a Bliss automated slide scanner to generate high-resolution digital images. The expression of COUP-TFII protein was scored and quantified as described previously[24,25]. In brief, the slides were digitized and nuclear COUP-TFII protein expression was scored and quantified based on a multiplicative index of the average staining intensity (0–3) and extent of staining (0–3) in the cores, yielding a 10-point staining index that ranged from 0 (no staining) to 9 (extensive, strong staining). Quantitative PCR (qPCR) was performed on RNAs isolated from patients with prostate cancer ($n = 36$) undergoing a radical prostatectomy for clinically localized prostate cancer with clinical characteristics as previously described[25]. The tissues were >70% cancerous based on histopathological analysis.

Animal experiments. All experiments were approved by the Animal Center for Comparative Medicine at Baylor College of Medicine. *COUP-TFII*$^{flox/flox}$ mice[7] were previously generated by our laboratory, and *COUP-TFII*$^{OE/+}$ mice were generated by our group using an approach as previously described[27]. *Pten*$^{flox/flox}$ mice[3] were obtained from H. Wu. The *ARR2PB-Cre* (PB-Cre) transgenic mice[28] were from F. Wang. The *Smad4*$^{flox/flox}$ mice[22] were from E. J. Robertson. PB-Cre, *COUP-TFII*$^{flox/flox}$, *COUP-TFII*$^{OE/+}$ and *Pten*$^{flox/flox}$ mice were backcrossed with C57BL/6 mice for at least five generations, and maintained according to the National Institutes of Health Guide for the Care and Use of Laboratory. *COUP-TFII*-floxed or *COUP-TFII*$^{OE/+}$ mice were first crossed with *Pten*-floxed or *Smad4*-floxed mice. The resulting compound mice were then crossed with PB-Cre mice for conditional knockout or overexpression of COUP-TFII in the prostate epithelium.

Expression plasmids and siRNA. The full-length human *COUP-TFII* cDNA was cloned into pMSCV-puro/neo (Clontech), pcDNA5 (Flag tag) (Invitrogen) and pcDNA3.1 (Myc tag) (Invitrogen) to generate COUP-TFII expression plasmids. Overlapping PCR with primers was used to generate Flag-COUP-TFII-M1 and M2 constructs, which are inserted in the KPNI/NheI sites of pcDNA5. Expression plasmids for epitope-tagged SMAD2/3/4, glutathione *S*-transferase (GST)-SMAD4 and the SMAD-binding element (SBE)-Luc reporter were described previously[29]. *COUP-TFII*-specific short hairpin RNA (shRNA) constructs were generated previously[30]. In brief, the shRNA for *COUP-TFII* (5′-AGGTAACGTGA TTGATTCAGTATCTTA-3′ and 5′-AGCTCTTGCTTCGTCTCCC-3′) was cloned into pSUPER.retro (OligoEngine). SMART pool or single siRNA duplexes targeting *COUP-TFII*, *Smad4* and control non-target siRNA were purchased from Dharmacon.

Cell culture and reagents. PC3, VCaP, LNCaP and DU145 cells were obtained from the ATCC and cultured in DMEM or RPMI supplemented with 10% fetal bovine serum. RWPE-1 cells (ATCC) were cultured with keratinocyte serum-free medium (K-SFM; Invitrogen) with bovine pituitary extract and human recombinant EGF. Cells were transfected with siRNA duplexes (40–80 nM) using lipofectamine (Invitrogen) or Dharmacon transfection (Dharmacon) reagents according to the manufacturer's instructions. COUP-TFII retrovirus was generated and transfected as previously described[1]. In brief, cells were transduced with retrovirus and cultured with 2 mg ml^{-1} puromycin or 400 mg ml^{-1} neomycin and the selection was stopped as soon as the non-infected control cells died off. Cell proliferation assay was performed using CellTiter 96 non-radioactive cell proliferation assay (MTT) kit (Promega) assay according to the manufacturer's instructions. Results were calculated based on three independent experiments and statistical significance was determined by two sided Student's *t*-test.

Luciferase reporter assay. Reporter assays were carried out as described[11]. In brief, 20–24 h after transfection, cells were treated with TGF-β (10 ng ml^{-1}) or SB431542 compound (20 nM) for 24 h. Cells were then collected for measurement of luciferase and β-galactosidase activities. All assays were done in duplicate and all values were normalized for transfection efficiency against β-galactosidase activities. Luciferase activity was determined with the Promega luciferase assay kit. Results were quantified based on three independent experiments and statistical significance was determined by two sided Student's *t*-test. *P* values less than 0.05 were considered significant.

RNA isolation and qPCR. Total RNA was extracted using TRIzol followed by the RNeasy mini kit (Qiagen) cleanup and RQ1 RNase-free DNase set treatment (Promega) according to the manufacturer's instructions. First-strand cDNA was synthesized using 2 μg of total RNA and Superscript II (Invitrogen). TaqMan universal master mix reagents and inventoried primer/probe mixtures (Applied Biosytems) were used for the reaction. Standard curves were generated by serial dilution of a preparation of total RNA, and all messenger RNA quantities were normalized against 18S RNA using ABI ribosomal RNA control reagents. The primers/probes used in this study are as follows: COUP-TFII (Mm00772789_m1), AR (Hs00171172_m1), probasin (Mm00444381_m1), NKX3.1 (Mm00440479_m1) and p21 (Hs00355782_m1). A Student's *t*-test was used for statistical analysis of qPCR results, and *P* values less than 0.05 were considered significant.

Histology and immunohistochemistry. The ventral, dorsolateral and anterior prostate lobes were dissected, fixed in 4% formaldehyde in PBS for 24 h, processed and embedded in paraffin. Sections (7 μm) were processed for H&E staining. Prostate hyperplasia is characterized by the proliferation of luminal cells with no cytological atypia, but contain small foci with two or three layers of cells. The PIN lesions were graded using the nomenclature and criteria developed previously[31]. In brief, high-grade PIN is characterized by an intraglandular proliferation of crowding cells with atypia, and cribriform formation or the development of multilayered solid glandular structures. Invasive adenocarcinoma is characterized by the proliferation of atypical cells that break the basal membrane and invade through the prostatic stroma. The quantitative results of tumour progression are from two random slides of each mouse in a total 10 pairs of the entire animal cohort. For immunohistochemistry, the slides were processed using a citrate-buffer-based antigen retrieval and the avidin–biotin peroxidase immunohistochemistry method. Sections were counterstained with 4′,6-diamidino-2-phenylindole (DAPI; Sigma-Aldrich). Quantification of tumour malignancy was done as follows: for Ki67 staining, positive cells were counted after imaging with a Zeiss Axioplan microscope. Three random slides for each animal were counted. The proliferative rate was determined by counting the proliferating cells (Ki67-positive) in a total of 100 cells, and the statistical significance was determined with a two-tailed Student's *t*-test. For lymph node metastasis, we performed CK8 or AR immunostaining in lymph nodes and recorded the percentage of mice that were positive for CK8 or AR, which we considered as lymph node metastasis. For invasive adenocarcinoma identification, we performed SMAα immunostaining. If the gland or acini displayed a loss or breakdown of the continuous layer of basal membrane (SMAα-positive) and the appearance of AR- or CK8-positive epithelial cells invading into the stromal compartment, we consider it as microinvasive cancer. The statistical significance between groups was determined with a two-tailed Fisher extract test.

Western blot and chromatin immunoprecipitation assay. Total proteins were extracted from cells following standard protocol[11]. Nuclear proteins were extracted using the NE-PER kit (Pierce). Protein concentration was measured using the BCA protein assay kit (Thermo Scientific). The primary antibodies used in this study were as follows: COUP-TFII (Perseus Proteomics), β-actin (Santa Cruz), phophorylated-H3 (Cell Signaling), PCNA (Santa Cruz), phospho-AKT403 (Cell Signaling), pan AKT (Cell Signaling), SMAD4 (Santa Cruz), p21 (BD), phospho-SMAD2 (Cell Signaling), SMAD2 (Zymed), SMAD3 (Zymed), cyclin D1 (Sigma), p15 (Santa Cruz) and p53 (Santa Cruz). Horseradish peroxidase (HRP)-conjugated secondary antibodies were purchased from DAKO. Signals were visualized with the Super Signal West Pico Chemiluminescent Substrate kit (Pierce). Chromatin immunoprecipitation assays were performed as described as previously[11] according to the protocol provided by Millipore. All the results are obtained from three independent samples and statistical significance was determined by a two-sided Student's *t*-test.

Immunoprecipitation and western blot analysis. Immunoprecipitation was performed as described previously[3]. Endogenous or epitope-tagged proteins were immunoprecipitated from cell lysates by the appropriate antibody affinity gel as indicated in the text and figure legends. After extensive washes, immunoprecipitated proteins were eluted in SDS sample loading buffer (Bio-Rad), separated by SDS–PAGE, transferred to nitrocellulose (Pierce) and detected in western blots with appropriate primary antibodies coupled with HRP-conjugated secondary antibody by chemiluminescence (Pierce).

GST fusion protein, *in vitro* protein binding and pull-down assays. GST fusion proteins were prepared using a commercial kit (Amersham Pharmacia Biotech). Target protein was pre-cleared with 5 μg of GST protein for 1 h and then incubated with 2 μg of various GST-fusion proteins for 2 h in the binding buffer (50 mM Tris-HCl, pH 7.5, 120 mM NaCl, 2 mM EDTA, 0.1% NP40). Proteins bound to GST-fusion proteins were retrieved on glutathione–sepharose beads, separated by SDS–PAGE and examined by western blot.

Electrophoretic mobility shift assay. Nuclear proteins from PC3 cells treated with TGF-β for 1 h were extracted using NE-PER kit (Pierce). Complementary oligonucleotides corresponding to the p21 SBE and its mutants were annealed and end labelled with [γ-^{32}P]ATP. The binding reactions were performed and analysed on a 5% non-denaturing gel. For supershift studies, 1 μg of antibody against SMAD4 (Santa Cruz) was preincubated for 20 min on ice, and DNA–protein complexes were visualized by autoradiography.

Microarray analysis. For microarray analysis, total RNA was isolated from control and COUP-TFII-knockdown PC3 cells. The Microarray Core at Baylor

College of Medicine performed the microarray hybridization with Affymetrix Human Genome U133 Plus 2.0. Gene information for all probes was annotated based on 'Human133_2.annot.csv' downloaded from the Affymetrix website. Raw data can be found in the GEO database as accession number GSE33182. The list of significance was operated by setting a false discovery rate (FDR) threshold at level of 0.05. All differentially expressed gene lists generated as described above were further analysed with the Ingenuity Pathways Analysis program (http://www.ingenuity.com/index.html) to identify canonical pathways, and molecular and cellular functions enriched in the related gene lists.

Clinical outcome analysis using GSE1064 data set. We defined a gene expression signature for COUP-TFII activity using an external human tumour data set and determined the correlation of COUP-TFII signature patterns with time to prostate cancer-specific death in patients. The COUP-TFII gene signature was derived from our own gene expression profile data set, of cells with or without COUP-TFII knockdown (GEO accession GSE33182, from ref. 21). The COUP-TFII gene signature (defined using fold change >1.5 for each *COUP-TFII* siRNA sample profile versus each control sample profile) consisted of 1,209 Affy probe sets (representing 829 unique genes) induced with COUP-TFII knockdown and 1,328 probe sets (891 genes) repressed with COUP-TFII knockdown (that is, the expression of 891 genes is induced by COUP-TFII, and 829 genes are repressed by COUP-TFII; Supplementary Data File). We used the previously described '*t*-score' metric[32–36] to define the COUP-TFII gene signature within profiles from an external human tumour data set (GEO accession GSE10645, using the 'human cancer panel', or GPL5858 platform). In brief, the *t*-score was defined for each external profile as the two-sided *t*-statistic comparing, within the profile, the average of the COUP-TFII-induced genes with the average of the COUP-TFII-repressed genes (genes within the GSE10645 data set were first centred to standard deviations from the median). The GSE10645 mRNA profile data set consisted of genes in a focused panel of 488 (which did not include *COUP-TFII* mRNA itself), of which 80 were represented in our COUP-TFII signature; for the 80 genes (47 induced by *COUP-TFII* siRNA and 33 repressed), the *t*-score contrasted the patterns of the COUP-TFII-induced genes against those of the COUP-TFII-repressed genes, to derive a single value denoting coordinate expression of the two gene sets (Supplementary Fig. 7). The univariate Cox proportional hazards analysis, multivariate Cox analysis, and Kaplan–Meier survival analysis were used to determine the correlation of COUP-TFII signature with patient outcome as described below. Furthermore, we performed a univariate analysis for each feature in the GSE10645 data set, and found the overall FDR to be reasonable. Out of 502 total features represented on the focused array, 131 had a univariate Cox $P < 0.01$, yielding an estimated FDR of $(502 \times 0.01)/131 = 3.8\%$. This indicates that there are widespread correlation patterns with outcome represented in the data set, similar to what one might find for other cancer profiling data sets. We also tested the ability of a random gene signature to predict outcome, using simulation testing in which *t*-scores were computed for each of 10,000 randomly generated signatures of the same gene number as the actual signature; for 95.8% of the random signatures, the correlation with worse patient outcome (as assessed by univariate Cox β value) did not exceed that for the actual signature.

Correlation of COUP-TFII signature with PSA recurrence. In addition to the GSE10645 (ref. 21) data set, we examined the signature in three other gene array data sets of human prostate tumours, from refs 37–39. In these other data sets, the outcome endpoint was PSA recurrence, whereas that for the GSE10645 data set was prostate-cancer-specific death. For multiple human tumour gene array data sets including GSE10645, we noted significant overlap between the genes repressed by COUP-TFII knockdown and the genes associated with worse outcome (Supplementary Table 4). However, when computing signature *t*-scores for each of the four data sets, the signature correlated with worse outcome for GSE10645 (ref. 21) (using prostate-cancer-specific death as the outcome measure) and ref. 37 data sets, but not with the refs 38 and 39 data sets, and not with time to PSA recurrence in the ref. 37 data set (Supplementary Table 5). Therefore, we conclude that the signature correlates with shorter time to prostate-cancer-specific death, with time to recurrence event having a weaker association.

Analysis of the enrichment of TGF-β-induced genes in COUP-TFII-depleted PC3 cells. A one-sided Fisher's exact test determined the significance of gene overlap between our COUP-TFII gene signature (as described above) and a previously generated gene signature of TGF-β activity (as reported previously[19]). Both data sets were generated using the Affymetrix U133 Plus 2 platform; therefore, the mapping between the two gene signatures was based on Affymetrix probe set identifier, with the gene population being the entire set (~54,675) represented on the gene array.

Statistical analysis. All experiments were performed using 3–15 mice or three independent repeated experiments from cells. Data are presented as mean and s.e.m. Spearman correlation coefficients were used to evaluate the relationships between COUP-TFII and clinicopathological variables or gene expression. The predictive value of COUP-TFII expression univariately with other clinical and pathological variables was analysed using the Cox proportional hazards regression model and the hazard ratio, and 95% confidence intervals were computed. The multivariate Cox proportional hazards model with the five-gene signature was used to estimate the coefficients of individual genes, which combined the five-gene expression levels into an integrated risk score model defined. Kaplan–Meier survival curves for different levels of COUP-TFII or COUP-TFII signature were also plotted. All analyses are performed with statistical software SPSS 19.0 (IBM, SPSS Statistics) or WinStat for Excel (R. Fitch software). Statistical significance was determined by a Student's *t*-test, Spearman correlation coefficients test, log-rank test or Fisher's exact test. For all statistical tests, the 0.05 level of confidence (two-sided) was accepted for statistical significance.

26. Agoulnik, I. U. *et al.* Androgens modulate expression of transcription intermediary factor 2, an androgen receptor coactivator whose expression level correlates with early biochemical recurrence in prostate cancer. *Cancer Res.* **66,** 10594–10602 (2006).
27. Wu, S. P., Lee, D. K., Demayo, F. J., Tsai, S. Y. & Tsai, M. J. Generation of ES cells for conditional expression of nuclear receptors and coregulators in vivo. *Mol. Endocrinol.* **24,** 1297–1304 (2010).
28. Wang, S. *et al.* Prostate-specific deletion of the murine Pten tumor suppressor gene leads to metastatic prostate cancer. *Cancer Cell* **4,** 209–221 (2003).
29. Feng, X. H., Liang, Y. Y., Liang, M., Zhai, W. & Lin, X. Direct interaction of c-Myc with Smad2 and Smad3 to inhibit TGF-β-mediated induction of the CDK inhibitor $p15^{Ink4B}$. *Mol. Cell* **9,** 133–143 (2002).
30. Li, L. *et al.* The nuclear orphan receptor COUP-TFII plays an essential role in adipogenesis, glucose homeostasis, and energy metabolism. *Cell Metab.* **9,** 77–87 (2009).
31. Park, J. H. *et al.* Prostatic intraepithelial neoplasia in genetically engineered mice. *Am. J. Pathol.* **161,** 727–735 (2002).
32. Creighton, C. J. *et al.* Integrated analyses of microRNAs demonstrate their widespread influence on gene expression in high-grade serous ovarian carcinoma. *PLoS ONE* **7,** e34546 (2012).
33. The Cancer Genome Atlas Research Network. Integrated genomic analyses of ovarian carcinoma. *Nature* **474,** 609–615 (2011).
34. Creighton, C. J. *et al.* Insulin-like growth factor-I activates gene transcription programs strongly associated with poor breast cancer prognosis. *J. Clin. Oncol.* **26,** 4078–4085 (2008).
35. Creighton, C. J. *et al.* Residual breast cancers after conventional therapy display mesenchymal as well as tumor-initiating features. *Proc. Natl Acad. Sci. USA* **106,** 13820–13825 (2009).
36. Luo, J. *et al.* A genome-wide RNAi screen identifies multiple synthetic lethal interactions with the Ras oncogene. *Cell* **137,** 835–848 (2009).
37. Glinsky, G. V., Glinskii, A. B., Stephenson, A. J., Hoffman, R. M. & Gerald, W. L. Gene expression profiling predicts clinical outcome of prostate cancer. *J. Clin. Invest.* **113,** 913–923 (2004).
38. Yu, Y. P. *et al.* Gene expression alterations in prostate cancer predicting tumor aggression and preceding development of malignancy. *J. Clin. Oncol.* **22,** 2790–2799 (2004).
39. Taylor, B. S. *et al.* Integrative genomic profiling of human prostate cancer. *Cancer Cell* **18,** 11–22 (2010).